JACC Vol. 25, No. 6
May 1995:1373–9

Comparison of Defibrillation Probability of Success Curves for an Endocardial Lead Configuration With and Without an Inactive Epicardial Patch

RICHARD L. CALLIHAN, MD, SALIM F. IDRISS, BSBME, ROGER W. DAHL, BSME, PATRICK D. WOLF, PHD, WILLIAM M. SMITH, PHD, RAYMOND E. IDEKER, MD, PHD, FACC

Durham, North Carolina

Objectives. **This study sought to assess the effect of passive "bystander" epicardial electrodes on defibrillation efficacy.**

Background. **We hypothesized that an inactive epicardial patch placed in an area of low potential gradient from an endocardial electrode shock might affect defibrillation efficacy through its effects on the shock field and the underlying potential gradient.**

Methods. **We studied the effects of an inactive 18-cm^2 titanium mesh patch placed on the anterolateral left ventricular epicardium on the 50% probability of successful defibrillation. A biphasic shock with both phases 6 ms in duration was delivered between superior vena cava and right ventricular catheter electrodes 10 s after the electrical induction of ventricular fibrillation. Six dogs underwent an up/down defibrillation protocol randomized with or without the patch on the heart.**

Results. **Mean 50% (±SD) probability point for energy doubled with the conductive patch on the heart, from 8.0 ± 3.2 to 16.8 ± 7.0 J ($p < 0.01$), and leading-edge voltage increased from 334 ± 64 to 477 ± 98 V ($p < 0.01$). Mean 50% probability points for energy and leading-edge voltage were not significantly changed when the procedure was repeated using a nonconductive patch in another six dogs as a control group. In a saline-saturated foam model, measurements from electrodes placed around and under the patch revealed a 72% mean decrease in the potential gradient in the foam under the conductive patch.**

Conclusions. **A passive defibrillator patch can markedly increase the energy requirements for defibrillation, probably by decreasing the potential gradient under the patch. These results suggest the use of caution when passive electrodes are present, for example, when a patient receives a nonthoracotomy defibrillator system while epicardial electrodes from a previously implanted system are left in place.**

(J Am Coll Cardiol 1995;25:1373–9)

Most theories of defibrillation mechanisms require that a minimal potential gradient be reached over all or a critical mass of the myocardium (1–6). Evidence suggests that the minimal potential gradient necessary to avoid regeneration of ventricular fibrillation in low-gradient areas is on the order of 3 to 10 V/cm (4,7–9). We hypothesized that a conductive epicardial electrode patch that is not connected to the defibrillator would create a region of very low potential gradient beneath it, which would adversely affect defibrillation thresholds. This could correspond to the clinical situation in which a defibrillator with transvenous leads is implanted in a patient in whom an epicardial patch is already in place but is not connected to a device. Using a canine model, we attempted to create such a current shunt or "short-circuit" pathway by placing a "bystander" patch on a part of the epicardium where the shock potential gradient field was already weak. We tested whether the inactive patch decreased the probability of successful defibrillation, presumably by altering the shock field. We also measured the potential gradients under and around the patch in a saline-saturated foam model to see whether the patch altered the shock field.

Methods

Defibrillation probability of success testing. The study was approved by the Institutional Animal Care and Use Committee at Duke University. It conformed to the "Position of the American Heart Association on Research Animal Use" adopted by the Association in November 1984.

Animal preparation. Anesthesia was induced in 12 mongrel dogs with intravenous pentobarbital (30 to 35 mg/kg body

From the Departments of Medicine and Pathology, Duke University Medical Center; Engineering Research Center for Emerging Cardiovascular Technologies; and Department of Biomedical Engineering, School of Engineering, Duke University, Durham, North Carolina. This study was supported in part by Research Grants HL-42760 and HL-44066 from the National Heart, Lung, and Blood Institute, National Institutes of Health, Bethesda, Maryland; Grant NC-93-SA-05 from the American Heart Association, Dallas, Texas; Grant CDR-8622201 from the National Science Foundation Engineering Research Center, Washington, D.C.; and by Cardiac Pacemakers, Inc., St. Paul, Minnesota. Mr. Dahl was a scientist at Cardiac Pacemakers, Inc. when this study was performed. Dr. Ideker is a consultant to companies that manufacture defibrillators.

Manuscript received May 6, 1994; revised manuscript received December 5, 1994, accepted December 15, 1994.

Address for correspondence: Dr. Raymond E. Ideker, University of Alabama at Birmingham, Volker Hall G82A, Box 201, Birmingham, Alabama 35294-0019.

0735-1097/95/$9.50
0735-1097(94)00558-8

weight) and maintained with a continuous infusion of pentobarbital at a rate of ~0.05 mg/kg per min. Succinylcholine (1 mg/kg) was also given intravenously at the time of anesthesia induction. Supplemental doses of succinylcholine (0.25 to 0.5 mg/kg) were given hourly as needed to maintain muscle relaxation. The animals were intubated with a cuffed endotracheal tube and ventilated with room air and oxygen through a Harvard respirator (Harvard Apparatus Co.). A peripheral intravenous line was inserted using sterile technique, and normal saline solution was infused continuously. A femoral artery line was placed for hemodynamic monitoring as well as arterial blood gas analysis and electrolyte measurements. Normal metabolic status was maintained by taking blood samples every 30 to 60 min and correcting any abnormal values. Electrocardiographic leads were applied for continuous monitoring of lead II. Body temperature was measured and maintained between 35°C and 37°C with a thermal mattress and heat lamp.

Electrodes. Using a transjugular approach, we advanced into the heart two 11F defibrillation catheters (Endotak, Cardiac Pacemakers Inc.) with a 3.7-cm^2 distal coil electrode 5 mm from the pacing electrode tip. Under fluoroscopic guidance, one catheter was positioned in the right ventricular apex as the anode for the first phase of the biphasic defibrillation shocks and as the stimulation catheter for the induction of fibrillation. The second catheter tip was positioned at the right atrial/superior vena cava junction as the cathode for the first phase of the biphasic defibrillation shocks. The chest was opened using a median sternotomy, and the heart was exposed and suspended in a pericardial cradle. Electrode position was then confirmed manually in all cases.

Fibrillation and defibrillation protocol. Ventricular fibrillation was induced by 60-Hz alternating current through the right ventricular apex defibrillation-catheter pacing electrode, grounded to the animal's chest wall. Fibrillation was allowed to continue for 10 s with the dog in end-expiration before attempting defibrillation. A failed shock was followed by a rescue shock of higher voltage delivered between the catheters. If the rescue shock failed, it was followed by internal paddle defibrillation using a Life-Pak 8 defibrillator (Physio-Control Corp.). A minimum of 4 min elapsed between each fibrillation–defibrillation attempt. Fibrillation was not reinitiated until blood pressure and heart rate had returned to normal. The defibrillation electrodes were connected to a defibrillator (HVS-02, Ventritex Inc.) that delivered a single-capacitor biphasic shock from a 150-μF capacitor bank. The truncated exponential biphasic shock used a second phase of opposite polarity to the first, with the second-phase leading-edge voltage equal to the first-phase trailing-edge voltage rounded to the nearest 10 V (Fig. 1). Each phase of the biphasic waveform was set at 6 ms with a 1-ms delay between phases. The actual current and voltage waveforms delivered to the electrodes were obtained by isolating and recording the voltage across a 0.25-Ω resistor in series with the electrodes and a 200:1,100-MΩ resistor divider in parallel with the electrodes. These waveforms were digitized at 20 kHz and recorded by a Data Precision 6100 waveform analyzer. Signal analysis software within the analyzer was used to calculate impedance and energy.

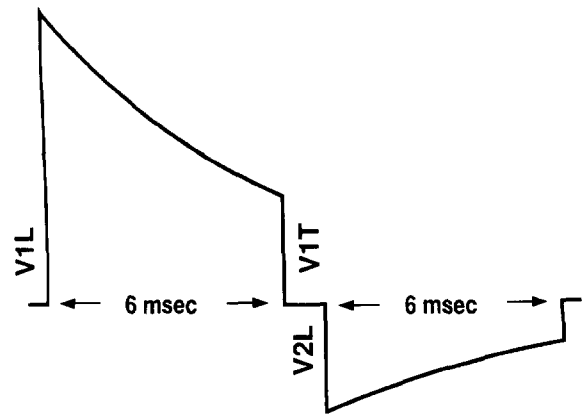

Figure 1. Diagram of a single-capacitor biphasic waveform. Voltage decreases exponentially for each waveform. Total duration of waveform is 12 ms. Leading-edge voltage of phase 2 (V2L) of the single-capacitor waveform equals trailing-edge voltage of phase 1 (V1T); polarity of V2L is opposite that of V1L.

Dose–response curves for defibrillation were measured in six animals with and without an 18-cm^2 titanium mesh patch placed on the anterolateral left ventricle. A second control group of six animals underwent an identical defibrillation protocol using a nonconductive patch that included 1-mm thick silastic insulation between the patch and the heart. The order in which the dose–response curves were determined (patch present or absent) was randomized. The patch was sutured to the epicardial surface of the anterolateral left ventricular free wall (Fig. 2), a region of low potential gradient for this electrode configuration (10), and the pericardial sac was reapproximated to improve patch contact with the heart. The patch remained disconnected from any electrical source during the study. We determined a dose–response curve (11–13) by

Figure 2. Schematic representation of the electrode distribution. One defibrillation electrode was positioned in the superior vena cava/right atrial (SVC/RA) junction, and the other was positioned in the right ventricular apex (RVA). The passive electrode patch was placed over the anterolateral left ventricular epicardium. LAD = left anterior descending coronary artery.

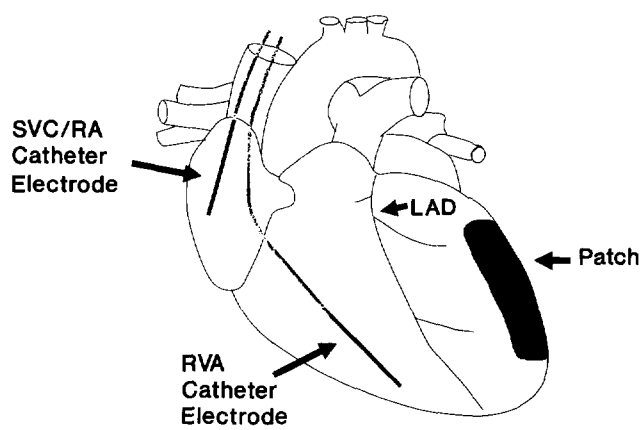

following a modified up/down protocol (14) that began with a leading-edge voltage of 500 V. The initial step size was 40 V. If the first shock failed, incremental 40-V shocks were tested until defibrillation was successful. If the first shock succeeded, decremental 40-V shocks were performed until the shock failed. After a reversal point was established, the step size was decreased to 20 V. After each successful shock the voltage was decreased by 20 V; after each unsuccessful shock it was increased by 20 V. This procedure was continued for a total of 20 shocks for trials with the patch on or with the patch off. At the end of the study euthanasia was induced with potassium chloride injection. The heart was removed and weighed. Probit analysis (15) was used to construct a probability of success curve from which 50% success levels of energy, leading-edge voltage and current were determined. Probability of success curves were generated for trials both with and without the patch.

In vitro potential gradient mapping. *Model.* An experimental model was constructed to assess the effects of an inactive electrode patch on a homogeneous potential gradient field. A rectangular foam sponge (12.5 × 15.0 × 4.5 cm) was placed in a plastic reservoir. A rectangular brass plate shocking electrode was placed at each end of the reservoir and pushed firmly against the ends of the sponge. The reservoir was then filled with normal saline solution to the top of the sponge. The foam sponge was squeezed repeatedly to remove all air bubbles from the material and to allow complete saturation of the foam with saline solution.

Thirty-two multielectrode arrays were placed on the top of the foam to map the potential gradient field created by shocks delivered to the brass plates. The arrays were distributed evenly over the surface of the foam, except in a region at the center where the inactive patch would be placed. In this region four arrays were positioned to measure the potential gradient beneath the patch. Additional arrays were placed at the edges of the patch region for more detailed mapping of this area (Fig. 3).

Electrodes. Each multielectrode array consisted of eight silver/silver chloride recording electrodes 127 μm in diameter with gold traces leading to 1-mm square bonding pads. The arrays were constructed using thin-film flexible circuit technology (16). A thin layer of gold was deposited on a sheet of 0.127-mm Kapton substrate. A computer-generated circuit design was then patterned on the substrate through selective photochemical etching of the gold layer. Solid silver was electroplated to gold recording sites and then chloridized to form a silver/silver chloride electrode (17).

Each array was used to measure the potential gradient at two sites. Each measurement site consisted of four electrodes arranged in a square with 4-mm diagonals (Fig. 4). The components of the potential gradient at each site were determined by dividing the measured potential change between electrodes along each of the diagonals by the interelectrode spacing. The magnitude of the two-dimensional potential gradient was then calculated by taking the square root of the sum of the squared potential gradient components.

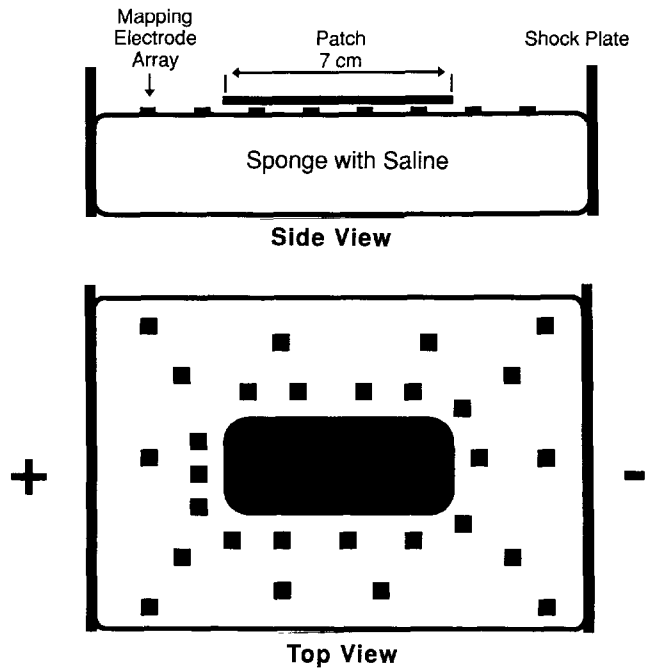

Figure 3. Diagram of the mapping experiment from side and top views. The patch is 7 cm long with 15 cm between the shock plates. The 32 electrode arrays with a total of 64 recording sites are positioned 0.5, 2.0 and 5.0 cm from the patch edge. Four electrodes are positioned 1.5 cm apart on the sponge beneath the patch.

Mapping protocol. Monophasic truncated exponential shocks of 10 ms were delivered to the foam model using a Ventritex HVS-02 defibrillator. Shocks (two each with leading edge of 50, 100 and 200 V) were first delivered while an 18-cm^2 oval patch of nonconductive plastic was placed on the surface of the foam in the central region (see explanation earlier). The plastic patch was then replaced with a stainless steel mesh patch with the same dimensions, and the shock protocol was repeated. During this procedure, 47 of 64 electrode recording

Figure 4. Diagram of the Kapton silver/silver chloride (Ag/AgCl) electrode array with 4 mm between opposite electrodes. Electrode diameter is 127 μm.

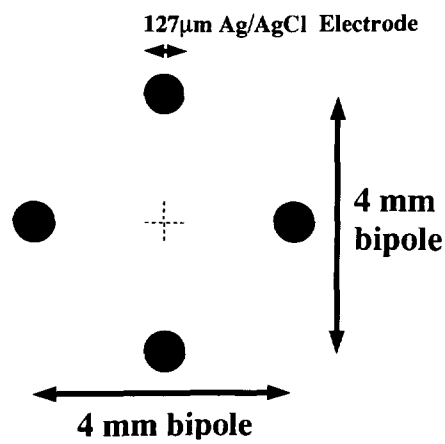

Table 1. Data for Six Study Dogs During Defibrillation Probability of Success Testing (50% success voltage, current and total energy with average impedance)

Dog	Patch	V	A	J	Ω
1	N	233	4.3	3.2	59.3
	Y	337	5.7	7.9	60.2
2	N	413	9.7	12.5	42.8
	Y	501	11.9	18.6	42.5
3	N	358	7.7	9.0	45.9
	Y	608	14.4	27.6	43.9
4	N	371	6.8	9.5	54.8
	Y	499	9.3	17.4	54.0
5	N	291	4.9	5.8	63.7
	Y	390	6.0	10.4	62.1
6	N	338	6.1	7.7	56.1
	Y	527	9.6	19.3	55.0
Mean ± SD	N	334 ± 64*	6.6 ± 2.0†	8.0 ± 3.2*	53.8 ± 8.0‡
	Y	477 ± 98	9.5 ± 3.4	16.9 ± 7.0	53.0 ± 8.2

*$p < 0.01$. †$p < 0.05$. ‡p = NS. N = no; Y = yes.

sites gave reproducible recordings and were used for potential gradient mapping.

For every shock delivered, differential voltages across diagonal electrodes of all multielectrode arrays were recorded using a multichannel cardiac mapping system (18). All measurements were made at a 2-kHz sampling rate. The components and magnitude of the two-dimensional potential gradient at each site were calculated using the peak measured differential voltages.

Statistical analysis. Results are expressed as mean value ± SD unless otherwise stated. Using the paired Student *t* test we compared the 50% probability points of the nonpatch trials with the patch trials in both sets of animals.

Results

Defibrillation probability of success with and without a patch. Table 1 shows the leading-edge voltage, current and total energy at the 50% probability point for study animals with and without the conductive patch. In each animal the patch increased the energy requirements by more than double from 8.0 ± 3.2 to 16.8 ± 7.0 J ($p < 0.01$). The mean leading-edge voltage increased significantly from 334 ± 64 to 477 ± 98 V ($p < 0.01$). The mean current increased from 6.6 ± 1.9 to 9.5 ± 3.4 A ($p < 0.05$). Table 2 shows the 50% success points for the voltage, current, and total energy in the control animals, which underwent the same protocol using a nonconductive patch. There was no statistical difference in any variables measured in the control group. Figure 5 shows the fitted probability of success curves for a single dog in the control group (Fig. 5, top) and one in the study group (Fig. 5, bottom). The curves for the control group dog nearly overlap each other; the study-group dog had a distinct shift of the patch curve to the right, indicating higher defibrillation voltage requirements for a given probability of success. Impedances were not statistically different with or without the conductive patch or the nonconductive patch (Tables 1 and 2).

Potential gradient mapping. Figure 6 shows three-dimensional contour plots of the potential gradient fields before and after the addition of the inactive conductive patch for a 100-V shock. A shock delivered to the model without the conductive patch created a relatively smooth potential gradient field with a magnitude of ~6 V/cm on the surface of the sponge (Fig. 6, left). However, addition of the inactive conductive patch severely distorted the potential gradient field both under and around the edges of the patch (Fig. 6, right). Beneath the conductive patch the potential gradient decreased to ~1 to 2 V/cm. At the edges of the patch closest to the shocking electrodes the potential gradient increased to ~10 to 15 V/cm. Similar changes in the potential gradient field were seen for the 50- and 200-V shocks.

At the edges of the patch closest to the shocking electrodes there was an increase in the potential gradient field on the surface of the foam. In contrast, the potential gradient field under the patch decreased far below the baseline level. This change in the potential gradient field under the patch is shown in Figure 7 as a function of shock voltage. For all three shock levels the conductive patch caused a significant ($p < 0.01$) decrease in the potential gradient magnitude under the patch, averaging 72 ± 13%.

Discussion

Major findings. We hypothesized that during endocardial defibrillation, a conductive epicardial patch might serve as a current shunt and in effect "short circuit" an area of epicardium underlying the patch. This could detrimentally alter the shock field by lowering the potential gradient in this area. Mapping studies (4,7,9,19) have demonstrated that in episodes of failed defibrillation, the earliest activations arise from the low gradient area and are responsible for the reinitiation of fibrillation. Therefore, an inactive electrode that decreases the shock field potential gradient could increase the voltage and energy required for defibrillation.

Table 2. Data for Six Control Dogs During Defibrillation Probability of Success Testing (50% success voltage, current and total energy with average impedance)

Dog	Patch	V	A	J	Ω
1	N	422	7.1	12.4	58.9
	Y	362	6.2	9.2	58.4
2	N	388	6.9	11.1	57.0
	Y	432	7.5	17.7	56.5
3	N	308	5.2	6.6	61.1
	Y	347	5.9	8.5	59.7
4	N	441	8.5	16.1	51.9
	Y	410	7.9	13.9	53.0
5	N	460	9.4	17.5	48.4
	Y	498	10.1	20.8	49.9
6	N	522	9.7	19.2	54.1
	Y	514	9.5	18.7	54.2
Mean ± SD	N	424 ± 72*	7.8 ± 1.7*	13.8 ± 4.7*	55.2 ± 4.7*
	Y	427 ± 69	7.9 ± 1.7	14.8 ± 5.1	55.3 ± 3.6

*p = NS. N = no; Y = yes.

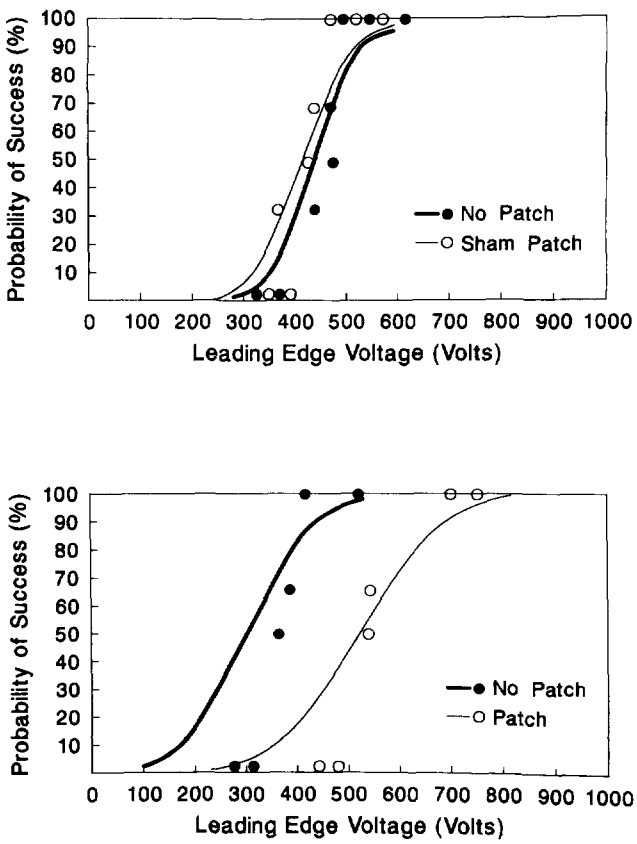

Figure 5. Probability of success curves for a dog from the control group **(top)** and one from the study group during defibrillation probability of success testing **(bottom)**. **Fitted curves** are shown for multiple trials with or without the patch.

We first performed defibrillation measurements in dogs with and without a passive conductive epicardial defibrillation patch electrode and found that defibrillation voltage, current and energy requirements are significantly higher with the patch present. This was not because the patch structurally or functionally altered the response of the heart to a shock because there was no difference in the defibrillation requirements for the control dogs with and without the nonconductive patch.

We investigated further the potential mechanism by which the patch could affect defibrillation efficacy. Potential gradient mapping in a foam model revealed a dramatic drop in the potential gradient magnitude under the patch, averaging 72% for the three shock intensities tested. The plaque caused an edge effect, with significantly increased gradients immediately outside its four corners and with the gradient beneath the patch quickly decreasing with distance inward from the edge. This gradient distribution supports the idea of a current shunt, with a high current density at the points where the current enters and leaves the patch. The depth to which the field is changed below the tissue–electrode interface is unknown.

Clinical implications. We believe that the shock electrode configuration played a significant role in our results and in the possible clinical implications of our findings. For a shock electrode configuration using superior vena cava and right ventricular apex endocardial catheters, the area of lowest potential gradient is the apicolateral region of the left ventricle (10). The patch was placed in an area that overlapped the low gradient region and extended high on the anterolateral left ventricular wall. Our intent in using a large defibrillation patch in the low gradient area was to maximize any effect on defibrillation efficacy by lowering the voltage gradient under the patch.

However, this patch position is near the location in which the left ventricular patch is placed in many patients during implantation of a defibrillator. Therefore, a secondary objective of the study was to simulate a clinical scenario in which patients who already have epicardial patches in place, with or without a defibrillator, are undergoing transvenous catheter lead placement for technical or medical reasons. Possible reasons for such a scenario include generator pouch/lead infection, patch lead fracture/failure, chronically elevated defibrillation thresholds with high failure rates and patch placement without a defibrillator at the time of left ventricular aneurysm resection, antiarrhythmic operation or other open-heart operative procedure (20–24).

For any of the previously mentioned clinical scenarios, the results of this study raise the possibility that endocardial lead placement in a patient with epicardial patches may significantly increase defibrillation requirements, in some cases to the extent that the device is unable to defibrillate successfully. It has been demonstrated that transthoracic defibrillation requirements are increased by the presence of large epicardial electrode patches in animals; some animals could not be defibrillated (25,26). Although one mechanism for this increased energy requirement for defibrillation may be exclusion of current through parts of the heart by the insulated portions of the patches, an additional mechanism may be shunting of the current through the conducting portions of the patches.

This study suggests that if epicardial patch electrodes are present these electrodes should be connected to the defibrillator whenever possible. Thus if a defibrillator is being replaced because of battery exhaustion or a defibrillator is being implanted for the first time in a patient who previously had patches placed, one should deliver the shocks through the patch electrodes rather than implanting one of the newer transvenous lead systems. However if a left ventricular patch electrode cannot be used, because of lead fracture for example, then the patch may have to be removed surgically unless an efficient waveform, such as one of the new biphasic waveforms, can achieve a defibrillation threshold with an adequate safety margin. A recent unpublished study suggested that a passive right ventricular electrode does not significantly increase defibrillation requirements (Fotuhi P, personal communication, September, 1994). Therefore, if the lead is fractured to the right ventricular patch, the study by Fotuhi, Idriss and Ideker suggests that it may be possible to defibrillate with a lead configuration consisting of the left ventricular patch already in place and a newly implanted right ventricular catheter electrode.

Another possible scenario in which a passive electrode may alter defibrillation requirements involves an electrode config-

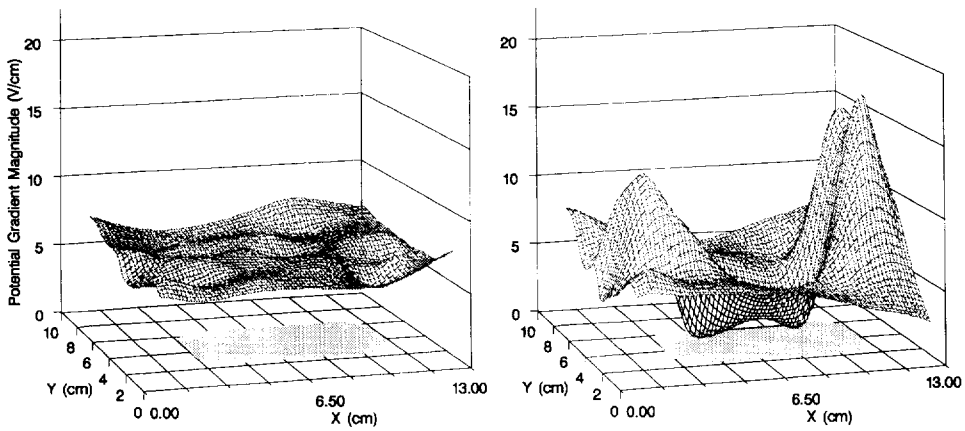

Figure 6. Three-dimensional representations of the potential gradient field on the surface of the sponge for a 100-V shock with and without the conductive patch. Each diagram was constructed from the measured potential gradients on the sponge using spline interpolation over an 80 × 48 grid of points. The **X and Y axes** at the bottom of each diagram are spatial coordinates in cm. The **shaded area** represents the patch. The shocking electrodes are located along the X = 0 cm and X = 15 cm lines. The potential gradient magnitude is graphed along the **Z axis. Left,** Potential gradient field of the surface of the sponge with a nonconductive patch in the central region. **Right,** Distortion present with a conductive patch.

uration that does not actively involve all electrodes present in or on the heart during a shock episode. When comparing the defibrillation efficacy of several different electrode configurations, many investigators have placed all electrodes to be tested in or on the heart at the beginning of the study (4,19,27–31). An inactive electrode during a defibrillation trial may alter the true threshold of other electrodes, possibly increasing it above the actual value.

Within the limitations of extrapolating data from an in vitro foam model to an animal model, it is reasonable to assume that the potential gradient drop under the patch in the foam model approximates the change seen in the animal study. Because the locations of the active and passive electrodes in this study were chosen to maximize the opportunity to detect differences in defibrillation success, defibrillation outcome and change in the shock field will probably differ with other electrode configurations. There was no overall effect upon the calculated resistance of the trials with the patch versus without the patch. Nonsignificant changes in impedance suggest that the fraction of the total shock current through the conductive patch is small; therefore small changes in the field can have large effects on defibrillation requirements.

Figure 7. Potential gradient magnitude under the patch for all three shock levels. The shock level is shown along the **X axis** and the potential gradient along the **Y axis**. Mean potential gradient magnitudes measured with and without the patch are shown. **Error bars** = 1 SD above the mean. Percent change in potential gradient with and without patch is shown as well. At each shock level there is a significant ($p < 0.01$) decrease in the potential gradient magnitude with the conductive patch.

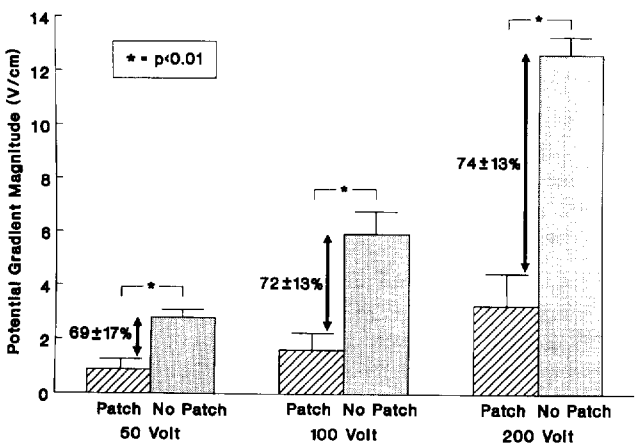

Conclusions. These results demonstrate that the presence of a passive defibrillator patch in a low gradient area during a cardiac defibrillation shock can significantly increase the voltage, current and energy necessary to achieve defibrillation. In a foam sponge model of uniform conductivity, a significant decrease in the measured potential gradient occurs under the patch when a shock is delivered. A decrease in the potential gradient under the patch in the animal could lead to an area of subthreshold potential gradient. A failed shock could occur secondary to post-shock activation fronts originating in the low gradient area, causing resumption of fibrillation. This could preclude the use of an endocardial lead configuration in clinical situations in which epicardial patches are already in place and should lead to special consideration in study design for testing multiple electrode configurations.

We thank Bruce Ash, MEE, at North Carolina State University for fabricating the multielectrode array wafers. We also thank Sharon Melnick, AAS, Ellen Dixon-Tulloch, MS, and Robert Walker, BA for technical assistance.

References

1. Wiggers CJ. The physiologic basis for cardiac resuscitation from ventricular fibrillation: method for serial defibrillation. Am Heart J 1940;20:413–22.
2. Zipes DP, Fischer J, King RM, Nicoll A, Jolly WW. Termination of ventricular fibrillation in dogs by depolarizing a critical amount of myocardium. Am J Cardiol 1975;36:37–44.
3. Chen P-S, Shibata N, Dixon EG, Martin RO, Ideker RE. Comparison of the

defibrillation threshold and the upper limit of ventricular vulnerability. Circulation 1986;73:1022–8.
4. Wharton JM, Wolf PD, Smith WM, et al. Cardiac potential and potential gradient fields generated by single, combined, and sequential shocks during ventricular defibrillation. Circulation 1992;85:1510–23.
5. Lepeschkin E, Jones JL, Rush S, Jones RE. Local potential gradients as a unifying measure for thresholds of stimulation, standstill, tachyarrhythmia and fibrillation appearing after strong capacitor discharges. Adv Cardiol 1978;21:268–78.
6. Tacker WA Jr, Bourland JD, Elam JA, Ewy GA, Langer A, Zoll P. Recommendations of the conference: IV. New directions in defibrillation. Med Instrum 1978;12:49–50.
7. Witkowski FX, Penkoske PA, Plonsey R. Mechanism of cardiac defibrillation in open-chest dogs with unipolar DC-coupled simultaneous activation and shock potential recordings. Circulation 1990;82:244–60.
8. Geddes LA, Niebauer MJ, Babbs CF, Bourland JD. Fundamental criteria underlying the efficacy and safety of defibrillation current waveforms. Med Biol Eng Comput 1985;23:122–30.
9. Zhou X, Daubert JP, Wolf PD, Smith WM, Ideker RE. Epicardial mapping of ventricular defibrillation with monophasic and biphasic shocks in dogs. Circ Res 1993;72:145–60.
10. Tang ASL, Wolf PD, Afework Y, Smith WM, Ideker RE. Three-dimensional potential gradient fields generated by intracardiac catheter and cutaneous patch electrodes. Circulation 1992;85:1857–64.
11. McDaniel WC, Schuder JC. The cardiac ventricular defibrillation threshold: inherent limitations in its application and interpretation. Med Instrum 1987;21:170–6.
12. Gold JH, Schuder JC, Stoeckle H. Contour graph for relating percent success in achieving ventricular defibrillation to duration, current, and energy content of shock. Am Heart J 1979;98:207–12.
13. Davy JM, Fain ES, Dorian P, Winkle RA. The relationship between successful defibrillation and delivered energy in open-chest dogs: reappraisal of the "defibrillation threshold" concept. Am Heart J 1987;113:77–84.
14. Bourland JD, Tacker WA Jr, Geddes LA. Strength-duration curves for trapezoidal waveforms of various tilts for transchest defibrillation in animals. Med Instrum 1978;12:38–41.
15. SAS/STAT User's Guide. Version 6, 4th ed, vol 2. Cary, NC: SAS Institute Inc., 1989:1324–50.
16. Mastrotatoro JJ, Massoud HZ, Pilkington TC, Ideker RE. Rigid and flexible thin-film multielectrode arrays for transmural cardiac recording. IEEE Trans Biomed Eng 1992;39:271–9.
17. Geddes LA, Baker LE, Moore AG. Optimum electrolytic chloriding of silver electrodes. Med Biol Eng 1969;7:49–56.
18. Wolf PD, Rollins DL, Blitchington TF, Ideker RE, Smith WM. Design for a 512 channel cardiac mapping system. In: Mikulecky DC, Clarke AM, editors. Biomedical Engineering: Opening New Doors. Proceedings of the Fall 1990 Annual Meeting of the Biomedical Engineering Society. New York: New York University Press, 1990:5–13.
19. Chen P-S, Wolf PD, Claydon FJ III, et al. The potential gradient field created by epicardial defibrillation electrodes in dogs. Circulation 1986;74: 626–36.
20. Watkins L, Platia EV, Mower MM, Griffith LSC, Mirowski M, Reid PR. The treatment of malignant ventricular arrhythmias with combined endocardial resection and implantation of the automatic defibrillator. Ann Thorac Surg 1984;37:60–5.
21. Platia EV, Griffith LSC, Watkins L Jr, et al. Treatment of malignant ventricular arrhythmias with endocardial resection and implantation of the automatic cardioverter-defibrillator. N Engl J Med 1986;314:213–6.
22. Winkle RA, Thomas A. The automatic implantable cardioverter defibrillator: the US experience. In: Brugada P, Wellens HJJ, editors. Cardiac Arrhythmias: Where to Go from Here? Mount Kisco, NY: Futura, 1987: 663–80.
23. Cox JL. Patient selection criteria and results of surgery for refractory ischemic ventricular tachycardia. Circulation 1989;79 Suppl I:I-163–77.
24. Olinger GN, Chapman PD, Troup PJ, Almassi GH. Stratified application of the automatic implantable cardioverter defibrillator. J Thorac Cardiovasc Surg 1988;96:141–9.
25. Walls JT, Schuder JC, Curtis JJ, Stephenson HE Jr, McDaniel WC, Flaker GC. Adverse effects of permanent cardiac internal defibrillator patches on external defibrillation. Am J Cardiol 1989;64:1144–7.
26. Lerman BB, Deale OC. Effect of epicardial patch electrodes on transthoracic defibrillation. Circulation 1990;81:1409–14.
27. Jones DL, Klein GJ, Guiraudon GM, et al. Internal cardiac defibrillation in man: pronounced improvement with sequential pulse delivery to two different lead orientations. Circulation 1986;73:484–91.
28. Fain ES, Sweeney MB, Franz MR. Sequential pulse internal defibrillation: is there an advantage to "switched" current pathways? Am Heart J 1989;118: 717–24.
29. Jones DL, Sohla A, Klein GJ. Internal cardiac defibrillation threshold: effects of acute ischemia. PACE 1986;9:322–31.
30. Chang MS, Inoue H, Kallok MJ, Zipes DP. Double and triple sequential shocks reduce ventricular defibrillation threshold in dogs with and without myocardial infarction. J Am Coll Cardiol 1986;8:1393–405.
31. Jones DL, Sohla A, Bourland JD, Tacker WA Jr, Kallok MJ, Klein GJ. Internal ventricular defibrillation with sequential pulse countershock in pigs: comparison with single pulses and effects of pulse separation. PACE 1987;10:497–502.